

# Quantitative characterization of optic nerve atrophy in patients with multiple sclerosis

Robert L Harrigan, Alex K Smith, Bailey Lyttle, Bailey Box, Bennett A Landman, Francesca Bagnato, Siddharama Pawate and Seth A Smith

Multiple Sclerosis Journal –  
Experimental, Translational  
and Clinical

July–September 2017: 1–8

DOI: 10.1177/  
2055217317730097

© The Author(s), 2017.  
Reprints and permissions:  
[http://www.sagepub.co.uk/  
journalsPermissions.nav](http://www.sagepub.co.uk/journalsPermissions.nav)

## Abstract

**Background:** Optic neuritis (ON) is one of the most common presentations of multiple sclerosis (MS). Magnetic resonance imaging (MRI) of the optic nerves is challenging because of retrobulbar motion, orbital fat and susceptibility artifacts from maxillary sinuses; therefore, axonal loss is investigated with the surrogate measure of a single heuristically defined point along the nerve as opposed to volumetric investigation.

**Objective:** The objective of this paper is to derive optic nerve volumetrics along the entire nerve length in patients with MS and healthy controls in vivo using high-resolution, clinically viable MRI.

**Methods:** An advanced, isotropic T2-weighted turbo spin echo MRI was applied to 29 MS patients with (14 patients ON+) or without (15 patients ON–) history of ON and 42 healthy volunteers. An automated tool was used to estimate and compare whole optic nerve and surrounding cerebrospinal fluid radii along the length of the nerve.

**Results and conclusion:** Only ON+ MS patients had a significantly reduced optic nerve radius compared to healthy controls in the central segment of the optic nerve. Using clinically available MRI methods, we show and quantify ON volume loss for the first time in MS patients.

**Keywords:** MRI, multiple sclerosis, axonal loss, atrophy

Date received: 8 March 2017; accepted: 1 August 2017

## Introduction

The human optic nerve is a small (<3 mm in diameter) white matter fiber bundle that exits the globe and courses posteriorly to the optic chiasm, and is responsible for communicating all visual stimuli to the optic tracts. It is immediately surrounded by cerebrospinal fluid (CSF) and sits inside the fatty tissue of the orbit superior to the maxillary sinuses. In patients with multiple sclerosis (MS), the optic nerve is one of the most common sites of injury. Approximately 25% of MS patients have retrobulbar optic neuritis (ON) as the first symptom and nearly two-thirds of MS patients experience at least one ON event in their lifetime.<sup>1</sup> ON is transient and may self-resolve in some cases or leave permanent damage in some others, though intervention with steroids has been shown to reduce the duration of symptoms.<sup>2</sup> Upon the acute phase resolution, ON leads to visual deficits in about 40%–60% of MS patients. The biological substrate of these visual

defects is unknown but axonal loss likely plays a major role.<sup>3</sup> This axonal loss is often investigated through optical coherence tomography using the surrogate of retinal nerve fiber layer thickness, which has been shown to correlate with disease severity because the loss of retinal axons is believed to be related to brain damage and atrophy.<sup>4</sup> However, this relationship is not well understood and offers only a surrogate for optic nerve axonal loss.

Magnetic resonance imaging (MRI) of the orbits represents a viable diagnostic tool for ON. In the acute phase, ON may present as an active lesion of the optic nerve on T1-weighted post-contrast sequences. This may leave a hyperintense lesion on T2-weighted MRI upon the resolution of the inflammatory event. Signal changes may be either focal or diffuse. Despite its clinical application, MRI of the orbits often turns out to be of little utility since signal alterations may not be visible even in the presence of

Correspondence to:  
**Robert L Harrigan**  
Vanderbilt University,  
Department of Electrical  
Engineering, 2301  
Vanderbilt Pl., PO Box  
351679 Station B, Nashville,  
TN 37235-1679, USA.  
[rob.l.harrigan@  
vanderbilt.edu](mailto:rob.l.harrigan@vanderbilt.edu)

**Robert L Harrigan**,  
Department of Electrical  
Engineering, Vanderbilt  
University, USA  
Vanderbilt University  
Institute for Imaging Science,  
Vanderbilt University, USA

**Alex K Smith**,  
Vanderbilt University  
Institute for Imaging Science,  
Vanderbilt University, USA  
Department of Biomedical  
Engineering, Vanderbilt  
University, USA  
Functional MRI of the Brain  
Centre, Nuffield Department  
of Clinical Neurosciences,  
University of Oxford, UK



**Bailey Lyttle,**  
Vanderbilt University  
Institute for Imaging  
Science, Vanderbilt  
University, USA

**Bailey Box,**  
Vanderbilt University  
Institute for Imaging  
Science, Vanderbilt  
University, USA

**Bennett A Landman,**  
Department of Electrical  
Engineering, Vanderbilt  
University, USA  
Vanderbilt University  
Institute for Imaging  
Science, Vanderbilt  
University, USA  
Department of Biomedical  
Engineering, Vanderbilt  
University, USA

**Francesca Bagnato,**  
Department of Neurology,  
Vanderbilt University  
Medical Center, USA

**Siddharama Pawate,**  
Department of Neurology,  
Vanderbilt University  
Medical Center, USA

**Seth A Smith,**  
Vanderbilt University  
Institute for Imaging  
Science, Vanderbilt  
University, USA  
Department of Biomedical  
Engineering, Vanderbilt  
University, USA  
Department of Radiology  
and Radiological Sciences,  
Vanderbilt University  
Medical Center, USA

a clear acute clinical event or chronic symptoms sequelae of tissue injury. Capturing axonal loss that ultimately results in optic nerve atrophy is virtually not possible. Measuring volume of the optic nerve is challenged by lack of contrast within the optic nerve and resolution sufficiently high to discriminate between the optic nerve and surrounding CSF.

Aside from MRI pulse sequences, a lack of robust analysis tools to characterize optic nerve atrophy cross-sectionally and over time have prevented accurate volumetric characterization of the optic nerve. Analyses typically proceeded by taking a single measurement of optic nerve size at a specified location along the nerve.<sup>5–8</sup> In this type of analysis, a single measurement is approximated as a surrogate for the health of the entire optic nerve and does not account for focal changes that may occur throughout the optic nerve length.

Recent advancements in MRI pulse sequences have offered improved contrast between the optic nerve and surrounding CSF while maintaining a relative insensitivity to motion (Figure 1). Our group has characterized these improvements in optic nerve MRI in healthy controls.<sup>9</sup> Additionally, we have recently developed an analysis pipeline for optic nerve MRI that affords an opportunity to evaluate the morphology of the optic nerve *in vivo* along its

entire length,<sup>10,11</sup> thereby allowing measurements of both global and focal atrophy.

To date, there has not been a systemic study of optic nerve morphological changes in patients with MS, to ascertain the amount of atrophy the optic nerve undergoes along its length after ON. As atrophy is directly tied to axonal loss, there is a need to understand optic nerve damage in MS accounting for local changes along the length of the optic nerve. We hypothesize that optic nerve volume loss can be detected and quantified in MS patients. Here, we report on the first automatic evaluation of optic nerve atrophy using advanced MRI in relapsing–remitting MS (RRMS) patients.

## Materials and methods

### Study design

This study is a collaborative project between the neuro-immunology division in the Neurology Department and the Institute of Imaging Science in the Radiology Department at Vanderbilt University Medical Center. The study was performed with approval of the Vanderbilt Institutional Review Board and signed informed consent was obtained prior to data acquisition from each participant. Patients were recruited from the Vanderbilt Multiple Sclerosis Clinic to participate in a separate

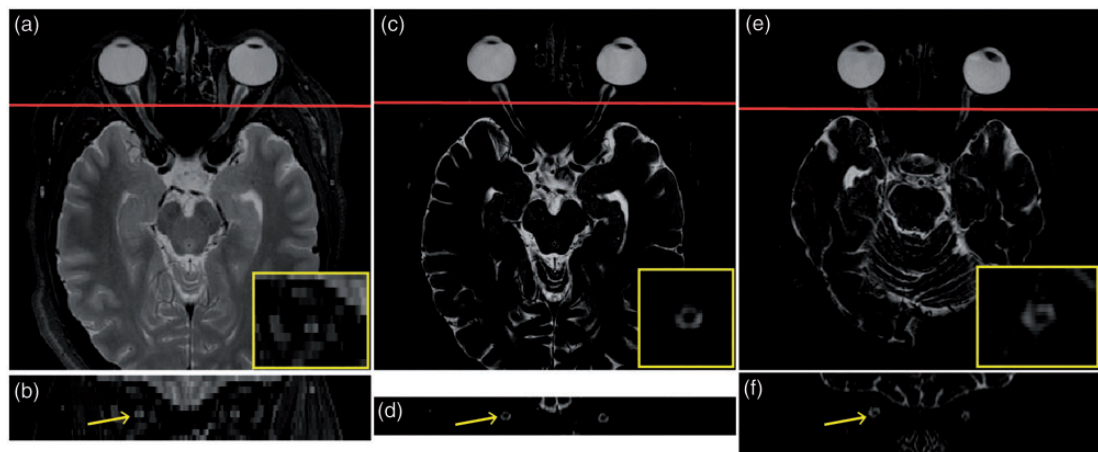


**Figure 1.** Healthy control scanned with: current clinical standard of care T2w MRI axial view (a) and coronal view approximately 10 mm posterior to the globe (b), as well as high-resolution isotropic T2w research imaging axial view (c) and coronal view approximately 10 mm posterior to the globe (d). One can appreciate the superior optic nerve:CSF contrast and benefits of isotropic resolution in visualizing optic nerve morphology in three dimensions. (e) and (f) show axial and coronal views of a 40-year-old RRMS patient with bilateral history of optic neuritis one year post-diagnosis. The regions indicated are enlarged in the yellow inlaid boxes for clarity.

T2w: T2-weighted; MRI: magnetic resonance imaging; CSF: cerebrospinal fluid; RRMS: relapsing–remitting multiple sclerosis.

research scan session independent of their clinical standard of care. All patients were diagnosed with RRMS by a neurologist. The presence or absence of ON was determined through chart review and confirmed by the attending ophthalmologist. We did not exclude patients who did not have optic nerve MRI findings, and relied on clinical evaluation and ophthalmological reports in the chart review. Patients who did not have confirmatory findings from an attending ophthalmologist were excluded from the study. Diagnosis of ON must have been noted within the previous five years.

### *MRI protocol*

Anatomical T2-weighted (T2w) VISTA (SPACE on Siemens, CUBE on GE) scans were obtained on one of two 3 Tesla (3T) Philips Achieva (Philips Medical Systems, Best, the Netherlands) scanners located in the Vanderbilt University Institute of Imaging Science using a two-channel body coil for transmission and an eight-channel head coil for reception. Importantly, both MRI scanners used in this study operated with the same hardware and software configurations. Images were acquired on the axial plane aligned with the optic nerve. Sequence parameters were: three-dimensional (3D) fast spin echo (repetition time/echo time/flip angle (TR/TE/ $\alpha$ ) = 4000 ms/404 ms/90 degrees), field of view =  $180 \times 180 \times 42 \text{ mm}^3$ , nominal resolution =  $0.6 \times 0.6 \times 0.6 \text{ mm}^3$ , Sensitivity Encoding (SENSE) factor = 2, fat saturation = spectral presaturation with inversion recovery (SPIR), and total scan time = 5:20 (appendix, Table 1).

### *Volumetric measurements*

We utilize a previously published, open source tool with minor modifications to automatically measure the radius of the optic nerve and surrounding CSF.<sup>12</sup> Briefly, this model fits an intensity profile to the optic nerve and CSF in the coronal plane and transforms the parameters from that fit into physical radius measurements. The model is applied to each coronal slice of the image containing the optic nerve and can therefore result in inconsistent measurements along the length of the optic nerve. To address this shortcoming we have modified this model by applying it in an iterative manner while decreasing the tolerance from adjacent slices.<sup>10</sup> This technique allows the model to ignore slices that are less than optimal and results in anatomically viable, 3D consistent measurements along the entire length of the optic nerve. This model is then applied to all of the patients and healthy volunteers, generating two sets of measurements for each individual.

### *Statistical analysis*

Volumetric data from the 42 pairs of nerves of the healthy control group were used to generate a normative distribution for detecting differences in patient sub-populations.<sup>9</sup> Group (patients vs healthy volunteers) differences in the optic nerve radius estimates were compared using a Wilcoxon rank-sum test. We use a previously published technique for comparing optic nerves across participants to overcome the differing number of measurements for each individual.<sup>9</sup> Measurements are interpolated to be the same length as the longest nerve among the population.

### **Results**

Twenty-nine MS (median age: 33; age range: 18–53; 69% female; 28 RRMS and one clinically isolated syndrome) and 42 healthy volunteers (median age: 28, age range: 20–38; 52% female) were enrolled in the study. Fourteen (48%) patients had no history of ON (namely ON–, hereafter). The remaining 15 patients had a history of either bilateral (seven patients) or unilateral (eight patients) ON (namely ON+, hereafter).

### *Qualitative results*

Figure 2 shows qualitative results for a healthy control ((a)–(c)) and a 47-year-old RRMS patient ((d)–(f)). The automatically segmented eye globes and optic chiasm are rendered in green and purple, respectively. The measurements for the optic nerve are rendered with color representing the nerve radius according to the color bar in (d).

### *Quantitative analysis*

Volumetrics of optic nerves that have never been affected by a clinical episode of ON ( $n=28$ ) were not significantly different from those derived from healthy controls (Figure 3, left). Involved nerves showed significantly reduced radius from healthy controls at 33% (16/48) of measurements localized in the central portion of the nerve and surviving Bonferroni correction (Wilcoxon rank-sum;  $p < 0.05$  Figure 3, right). Of these differences, 15 were continuous points in the central portion of the nerve (Figure 3, right: shaded area), the last point that is significantly different from the healthy controls is posterior to the shaded region, separated by a single non-significant point.

### **Discussion**

We present the first analysis of optic nerve radius using advanced MRI along the entire length of the nerve as it applies to patients with MS and ON. In the present work, we used a T2w

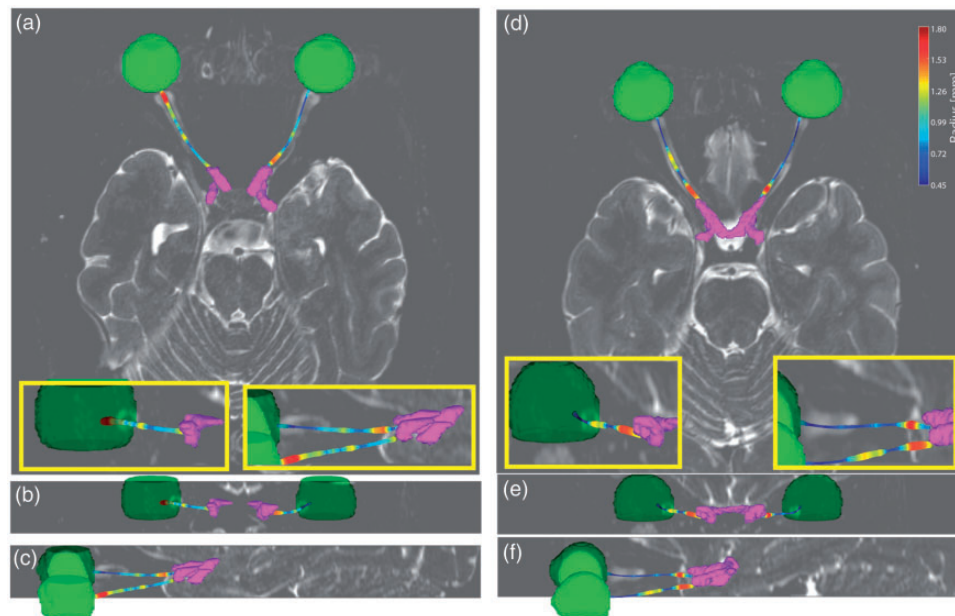


**Figure 2.** Renderings of the segmented eye globes (green) and optic chiasm (purple) along with the measured optic nerves for a healthy control ((a)–(c)) and a 47-year-old relapsing–remitting multiple sclerosis patient 15.5 years post-diagnosis with a history of optic neuritis in the left eye ((d)–(f)). Color of the optic nerve corresponds to estimated optic nerve radius in all panels according to the color bar in (d). Optic nerve atrophy can be clearly seen in ((d)–(f)) as compared to ((a)–(c)). (b), (c), (e) and (f) are enlarged in the yellow inlaid boxes for clarity.

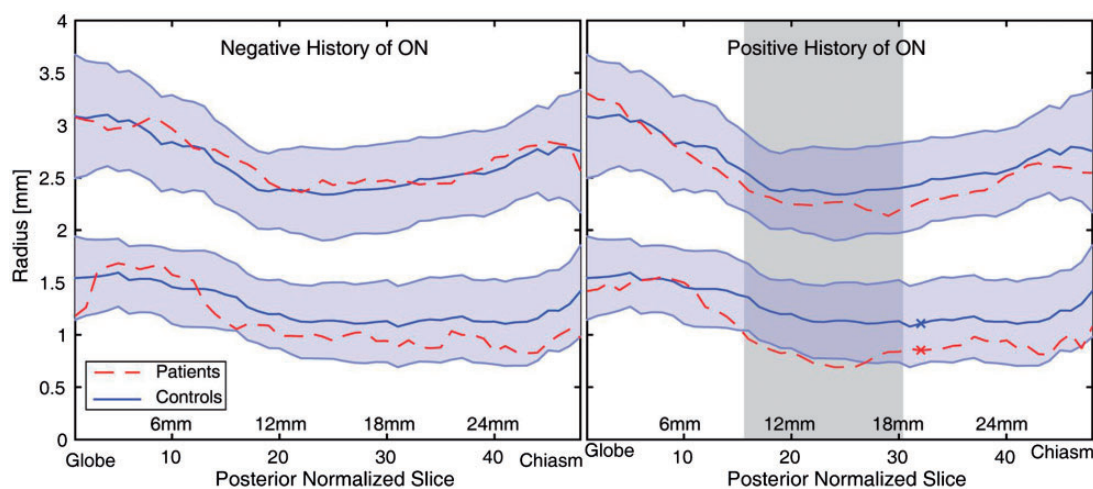


**Figure 3.** Comparison of volumes of optic nerves never affected by optic neuritis (ON) (left) and optic nerves with a previous history of ON (right) to healthy controls. The upper distribution is the diameter of the sub-arachnoid cerebrospinal fluid while the lower line is the radius of the optic nerve. The shaded blue region indicates one standard deviation of the healthy control population. The shaded region (right) illustrates the region of 15 consecutive measurements (9 mm) where the patients' nerves are significantly smaller than healthy nerves (Wilcoxon rank-sum;  $p < 0.05$  Bonferroni corrected). The nerves from patients with a negative history of ON were not significantly different from healthy controls.

turbo spin echo (TSE) sequence with extended echo train. The advantage of this sequence over currently available ones is the superior resolution and nerve/CSF contrast. It also shows a clinically affordable acquisition time<sup>11</sup> (Figure 1 (a)–(d)). The isotropic resolution allows for accurate 3D characterization of the optic nerve from globe to chiasm.

Our data detected for the first time a group-level atrophy effect on nerves affected by ON as compared to optic nerves that have never been affected by disease. This analysis is superior to traditional single-point metrics that have traditionally been used to characterize optic nerve atrophy as this technique can provide more insight into focal optic nerve changes. As such this technique has the potential to provide a greater understanding of the degree and location of axonal loss that is known to be associated with ON.

The finding of significant atrophy in only the central part of the nerve, as opposed to the entire length of the nerve, is possibly an artifact of the fact that measurement accuracy is the highest in the central portion of the nerve; the anterior and posterior portions each presents its own challenges. The anterior portion of the nerve is difficult to characterize accurately because of motion artifacts from saccadic eye movements. The posterior region of the nerve is difficult to characterize as the sub-arachnoid CSF thins as the nerve approaches the optic chiasm. This thinning of CSF reduces the contrast available for accurately measuring the nerve. These challenges may be preventing accurate estimation of the anterior and posterior portions of the nerve, masking significant differences among patients. Further technical improvements and increased sample size can lend insight into this phenomenon.

Although novel, our work is not exempt from limitations. In the future it could be improved on by accounting for the curvature of the optic nerve in the interpolation step. Interpolating nerves to be the same length results in a coarse alignment of nerves across the population but does not account for varying curvature across individuals. Investigation into the most appropriate alignment methods is still required.

Our method is also resolution dependent, which limits the number of patients that can be enrolled in these studies since it cannot be applied to clinical standard of care imaging protocols. If the method were to be extended to work on multiple or lower

resolutions while maintaining comparable accuracy, study sizes could increase.

Notwithstanding the above limitations, we believe that our work represents a preliminary but solid demonstration of volumetric measurements of the optic nerve in its entire length. This proof of concept could lead to a tool that quantitatively assesses a patient's severity of ON atrophy, prognosis or treatment approach. With future work this methodology may translate into clinical application and can provide useful information on the disease stage and course in patients with a history of ON whose symptoms often do not find a biological surrogate.

### Acknowledgments

All tools used and developed in this work are available in open source from their respective authors. The optic nerve/CSF estimation code is primarily written in MATLAB (The MathWorks Inc, Natick, MA, USA) and bundled into an automated program (i.e. “spider”<sup>13</sup>) that combines these tools using PyXNAT<sup>14</sup> for XNAT<sup>15</sup> and is available in open source through the NITRC project MASIMATLAB (<http://www.nitrc.org/projects/masimatlab>).

### Conflicts of interest

The author(s) declared no potential conflicts of interest with respect to the research, authorship, and/or publication of this article.

### Funding

The author(s) disclosed receipt of the following financial support for the research, authorship, and/or publication of this article: Research reported in this publication was supported in part by the National Institutes of Health R21EY024036, R01EY023240 and 5T32EY007135. The content is solely the responsibility of the authors and does not necessarily represent the official views of the National Institutes of Health. This project was supported in part by ViSE/VICTR VR3029. The project described was supported by the National Center for Research Resources, Grant UL1 RR024975-01, and is now at the National Center for Advancing Translational Sciences, Grant 2 UL1 TR000445-06. This work was conducted in part using the resources of the Advanced Computing Center for Research and Education at Vanderbilt University, Nashville, TN.

### Supplementary material

Supplementary material is available for this article online.

## References

1. Optic Neuritis Study Group. Multiple sclerosis risk after optic neuritis: Final optic neuritis treatment trial follow-up. *Arch Nives of neurology* 2008; 65: 727–732.
2. Beck RW, Cleary PA, Anderson MM Jr, et al. A randomized, controlled trial of corticosteroids in the treatment of acute optic neuritis. *N Engl J Med* 1992; 326: 581–588.
3. Optic Neuritis Study Group. Visual function 15 years after optic neuritis: A final follow-up report from the Optic Neuritis Treatment Trial. *Ophthalmology* 2008; 115: 1079–1082.e5.
4. Abalo-Lojo JM, Limeres CC, Gómez MA, et al. Retinal nerve fiber layer thickness, brain atrophy, and disability in multiple sclerosis patients. *J Neuroophthalmol* 2014; 34: 23–28.
5. Hickman S, Toosy A, Jones S, et al. Serial magnetization transfer imaging in acute optic neuritis. *Brain* 2004; 127: 692–700.
6. Lagrèze WA, Gaggli M, Weigel M, et al. Retrobulbar optic nerve diameter measured by high-speed magnetic resonance imaging as a biomarker for axonal loss in glaucomatous optic atrophy. *Invest Ophthalmol Vis Sci* 2009; 50: 4223–4228.
7. Yiannakas MC, Wheeler-Kingshott CA, Berry AM, et al. A method for measuring the cross sectional area of the anterior portion of the optic nerve in vivo using a fast 3D MRI sequence. *J Magn Reson Imaging* 2010; 31: 1486–1491.
8. Lenhart PD, Desai NK, Bruce BB, et al. The role of magnetic resonance imaging in diagnosing optic nerve hypoplasia. *Am J Ophthalmol* 2014; 158: 1164–1171.e2.
9. Harrigan RL, Plassard AJ, Mawn LA, et al. Constructing a statistical atlas of the radii of the optic nerve and cerebrospinal fluid sheath in young healthy adults. *Proceedings of SPIE—the International Society for Optical Engineering*. Vol. 9413. NIH Public Access, 2015.
10. Harrigan RL, Smith AK, Mawn LA, et al. Improved automatic optic nerve radius estimation from high resolution MRI. *Proc SPIE Int Soc Opt Eng* 2017; 101331C–101331C.
11. Harrigan RL, Smith AK, Mawn LA, et al. Short term reproducibility of a high contrast 3-D isotropic optic nerve imaging sequence in healthy controls. *Proceedings of SPIE—the International Society for Optical Engineering*. Vol. 9783. NIH Public Access, 2016.
12. Harrigan RL, Plassard AJ, Bryan FW, et al. Disambiguating the optic nerve from the surrounding cerebrospinal fluid: Application to MS-related atrophy. *Magn Reson Med* 2016; 75: 414–422.
13. Gao Y, Burns SS, Lauzon CB, et al. Integration of XNAT/PACS, DICOM, and research software for automated multi-modal image analysis. *Proceedings of SPIE*. Vol. 8674. NIH Public Access, 2013.
14. Schwartz Y, Barbot A, Thyreau B, et al. PyXNAT: XNAT in Python. *Front Neuroinform* 2012; 6: 12.
15. Marcus DS, Olsen TR, Ramaratnam M, et al. The Extensible Neuroimaging Archive Toolkit: An informatics platform for managing, exploring, and sharing neuroimaging data. *Neuroinformatics* 2007; 5: 11–34.

**Appendix Table 1.** MS Journal Appendix for MRI methodology.

Hardware		
Field strength	3T	
Manufacturer	Philips	
Model	Achieva	
Coil type (e.g. head, surface)	Head	
Number of coil channels	8	
Acquisition sequence		
Type (e.g. FLAIR, DIR, DTI, fMRI)	3D Turbo spin echo	
Acquisition time	7:48	
Orientation	Transverse	
Alignment (e.g. anterior commissure/ poster commissure line)	Localized SI along the optic nerve	
Voxel size	0.55 mm isotropic	
TR	4000 ms	
TE	455 ms	
TI	N/A	
Flip angle	90°	
NEX	2	
Field of view	180 × 180 × 20 mm <sup>3</sup>	
Matrix size	328 × 328	
Parallel imaging	<b>Yes</b>	<b>No</b>
If used, parallel imaging method: (e.g. SENSE, GRAPPA)	SENSE = 2	
Cardiac gating	Yes	<b>No</b>
If used, cardiac gating method: (e.g. PPU or ECG)	N/A	
Contrast enhancement	Yes	<b>No</b>
If used, provide name of contrast agent, dose and timing of scan post- contrast administration	N/A	
Other parameters:		
	Recon Matrix = 512	
	TSE factor = 70	
	Turbo direction = radial	
	SPIR strength = strong	
Image analysis methods and outputs		
Lesions		
Type (e.g. Gd-enhancing, T2-hyperintense, T1-hypointense)		
Analysis method		
Analysis software		
Output measure (e.g. count or volume [ml])		
Tissue volumes		
Type (e.g. whole brain, grey matter, white matter, spinal cord)		
Analysis method		
Analysis software		
Output measure (e.g. absolute tissue volume in ml, tissue volume as a fraction of intracranial volume, percentage change in tissue volumes)		

(continued)

**Appendix Table 1.** Continued

Tissue measures (e.g. MTR, DTI, T1-RT, T2-RT, T2\*, T2', <sup>1</sup>H-MRS, perfusion, Na)

Type (e.g. whole brain, grey matter, white matter, spinal cord, normal-appearing grey matter or white matter)

Analysis method

Analysis software

Output measure

Other MRI measures (e.g. functional MRI)

Type (e.g. whole brain, grey matter, white matter, spinal cord, normal-appearing grey matter or white matter)

Analysis method

Analysis software

Output measure

**Other analysis details:**

FLAIR: fluid-attenuated inversion recovery; DIR: double inversion recovery; DTI: diffusion tensor imaging; fMRI: functional magnetic resonance imaging; 3D: three-dimensional; SI: superior-inferior; TR: repetition time; TE: echo time; TI: inversion time; NEX: number of excitations; SENSE: Sensitivity Encoding; GRAPPA: Generalized Autocalibrating Partial Parallel Acquisition; PPU: peripheral pulse unit; ECG: electrocardiogram; TSE: turbo spin echo; SPIR: spectral presaturation with inversion recovery; Gd: gadolinium; MTR: magnetization transfer ratio; DTI: diffusion tensor imaging; RT: relaxation times; <sup>1</sup>H-MRS: proton magnetic resonance spectroscopy; MRI: magnetic resonance imaging; fMRI: functional magnetic resonance imaging.